DOI: https://doi.org/10.26896/1028-6861-2023-89-1-67-73

A WALKER-BASED MEAN STRAIN CORRECTION MODELS FOR LOW-CYCLE FATIGUE LIFE PREDICTION

© **Anton N. Servetnik**

Central Institute of Aviation Motors, 2, Aviamotornaya Street, Moscow, 111116, Russia; e-mail: anservetnik@ciam. ru

Received June 8, 2022. Revised August 25, 2022. Accepted September 29, 2022.

A Walker-based mean strain correction model of low-cycle fatigue (LFC) life prediction is proposed for high loaded parts. The model is based on a function depending on the strain range and strain ratio controlled in the strain-controlled LCF test of fatigue specimens and a constant reflecting the material sensitivity to strain ratio. The independence from the stress cycle parameters which can change during the strain-controlled LCF test is an obvious advantage of the model. The model was verified using the results of strain-controlled LCF tests of smooth titanium alloy Ti-6Al-4V ELI and iron-based alloy specimens conducted at room temperature. The proposed model was compared to the Smith – Watson – Topper and Walker models that take into account the mean stress effect. The proposed model provided the best prediction accuracy for titanium alloy. For Iron-based alloys the results obtained by the Walker model and the model proposed are close to each other. A simplified model based on the analysis of model parameters taking into account the mean strain effect for predicting fatigue life of aeroengine critical parts is developed using a limited amount of experimental data when only the results of $R_\varepsilon = 0$ tests are known. A comparison of the predicted life with the number of cycles to failure showed satisfactory results of fatigue life prediction for Ti-6Al-4V ELI and Iron-based alloys specimens.

Keywords: low cycle fatigue; fatigue life prediction; strain-life curve; SWT model; Walker model; mean strain; strain-controlled test.

INTRODUCTION

Large number of parts are subjected to cyclic loads, resulting in cyclic stresses and strains in the parts. Crack initiation and failure of parts usually happens in LCF region ($\sim 10^2 - 10^5$ cycles) with elastoplastic deformation in local stress concentration zones. Depending on the part design and combination of external loads, the stresses and strains can be non-symmetrical.

It is known that loading cycle asymmetry is one of the factors having the most impact on fatigue life. The fatigue life of a part in stress concentration zones is estimated using strain-life LCF curves tested in similar or more severe conditions. In this case, the fatigue life estimate is considered conservative.

The strain cycle is characterized by the maximum ε_{max} and minimum ε_{min} cycle strains or the strain range $\Delta\varepsilon = \varepsilon_{max} - \varepsilon_{min}$ and the mean strain $\varepsilon_m = (\varepsilon_{max} + \varepsilon_{min})^2$ (Fig. 1). The strain ratio is the ratio of the minimum strain to the maximum strain $R_\varepsilon = \varepsilon_{min}/\varepsilon_{max}$.

It is known that the strain-life LCF curve can be significantly affected by the material properties and material testing conditions. In this paper, to simplify the LCF model a power law equation of the strain range vs. number of cycles to failure N_f was used [1]

$$\Delta\varepsilon = AN_f^b \tag{1}$$

or its linearized form

$$\log N_f = -\frac{1}{b}\log A + \frac{1}{b}\log \Delta\varepsilon, \tag{2}$$

where A and b are the fatigue coefficient and exponent.

In strain-controlled tests the parameters of the strain cycle are the controlled variables, while the

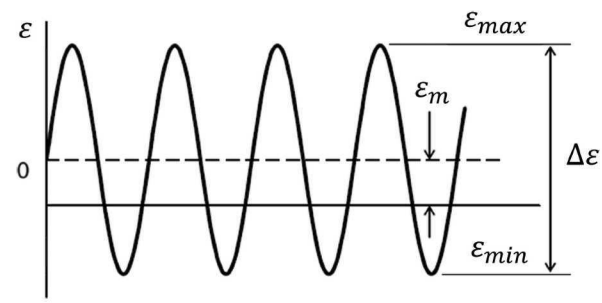

Fig. 1. Strain cycle parameters

number of cycles to failure is an independent (random) variable. The parameters of the stress cycle, like stress range $\Delta\sigma$ and mean stress σ_m, are dependent variables, whose values may change during the test. Usually for constructing the LCF curve with mean stress effect the maximum stress σ_{max} corresponding to the cycle with stabilized hysteresis loop or the value for the half of cycles to failure $\sigma_{max} = \sigma_{max}(N_f/2)$ is used.

The relationship between the number of cycles to failure and the parameters of the strain cycle is established based on a series of tests of standard smooth specimens for different values of strain range $\Delta\varepsilon$ and strain ratio R_ε. Strain-life LCF curves for different R_ε are constructed via regression analyses of the test results.

For estimating the life of a part using strain-controlled test results strain range and stress ratio are used. If the stress ratio of part loading and the stress ratio from the test do not match, then the LCF curve with desired strain ratio can be obtained based on a model of a LCF cycle mean stress effect. This model is based on a function of the number of cycles to failure, strain range and stress ratio.

Different models were developed to account for mean stress effect like Morrow [2], Smith – Watson – Topper (SWT) [3], Walker [4], modified by Morrow, SWT, and Walker [5 – 16]. The Morrow model [2] takes into account the mean stresses mostly in the high-cycle fatigue region. The Morrow model, modified by Manson and Halford [5], usually overestimates LCF life, and it is only applicable for steels [11]. For estimating LCF life the SWT and Walker models, as well as their modifications, have been used most often [14 – 17, 20], because they give a good life estimate for many materials [21, 22].

The SWT-based fatigue life prediction model with mean stress effect is described by the following equation

$$\varepsilon_{SWT} = \sigma_{max}\Delta\varepsilon = AN_f^b \qquad (3)$$

or its linearized form

$$\log N_f = -\frac{1}{b}\log A + \frac{1}{b}\log \sigma_{max} + \frac{1}{b}\log \Delta\varepsilon. \qquad (4)$$

The SWT model is based on the hypothesis of the constant potential strain energy density for the given life. The model assumes that the parameter ε_{SWT} is constant for any combinations of σ_{max} and $\Delta\varepsilon$. For constructing the SWT model only the results for fully reversed tests are used, so it is convenient to use this model in practice when there are no mean stress cycle test results.

The Walker-based fatigue life prediction model with mean stress effect is given by [17]

$$\varepsilon_w = \left(\frac{\sigma_{max}}{E}\right)^{1-w} (\Delta\varepsilon)^w = AN_f^b. \qquad (5)$$

The linearized form of this model is given by

$$\log N_f = -\frac{1}{b}\log A + \frac{w}{b}\log \Delta\varepsilon + \frac{1-w}{b}\log \frac{\sigma_{max}}{E}, \qquad (6)$$

where E is the elasticity modulus, determined directly from an LCF test from the loading branch of the hysteresis loop and w is the Walker fitting constant.

The formulation of the Walker-based model (5) was derived from the classical Walker model [4]

$$\sigma_w = (\sigma_{max})^{1-w}(\Delta\sigma)^w. \qquad (7)$$

This formulation was obtained by dividing both sides of the expression by the elasticity modulus and replacing $\Delta\sigma/E$ with $\Delta\varepsilon$. This transition is not valid from the standpoint of inelastic deformation, however, expression (5) can now be represented in a simple and easy-to-calculate form. The Walker model is based on the assumption that the influence of mean stresses on fatigue differs from material to material. Thus, the constant w varying from 0 to 1 determines material sensitivity to the stress ratio. The smaller w, the more a material is sensitive to the stress ratio. For $w = 0.5$ the Walker model transforms in the SWT model.

When the parameters A, b, and w of Eq. (6) are calculated from regression analysis, the input data includes both the results from fully reversed and mean strain cycle tests. So, the Walker-based models describe material performance for a wide range of stress ratios better than Morrow and SWT models.

The proposed mean strain correction model

From the strain-controlled test results one acquires the controlled parameters like the strain range and strain ratio. The parameters of the stress cycle may vary and not always available for analysis. The models considered in the previous section do not take into account strain ratio. The proposed model in represented in the form of a function of two parameters of a strain-controlled test, strain range and strain ratio [23], and also incorporates the constant w_ε that adjusts for the material sensitivity to strain ratio

$$\varepsilon_w = f(\Delta\varepsilon, R_\varepsilon, w_\varepsilon). \qquad (8)$$

This relationship is obtained by dividing both sides of Eq. (7) by elasticity modulus and replacing σ_{max}/E with ε_{max} and $\Delta\sigma/E$ with $\Delta\varepsilon$:

$$\varepsilon_w = \varepsilon_{max}^{1-w_\varepsilon} \Delta\varepsilon^{w_\varepsilon} = \Delta\varepsilon \left(\frac{1}{1-R_\varepsilon} \right)^{1-w_\varepsilon}. \quad (9)$$

Like the Walker model (5), model (9) is not correct for inelastic deformation. However, model (9) accounts for the strain ratio and the material sensitivity to the strain ratio.

A mean strain correction LCF model incorporated in power law equation is formulated as follows

$$\varepsilon_w = \Delta\varepsilon \left(\frac{1}{1-R_\varepsilon} \right)^{1-w_\varepsilon} = AN_f^b. \quad (10)$$

The linearized form is given by

$$\log N_f = -\frac{1}{b}\log A + \frac{1}{b}\log\Delta\varepsilon + \frac{1-w_\varepsilon}{b}\log\frac{1}{1-R_\varepsilon}. \quad (11)$$

The limitation of the model is the condition of pure compression ($\varepsilon_{max} \le 0$). The constants A, b, and w_ε of Eq. (11) are determined using two-factor linear regression analysis, where both the results of fully reversed and non-fully reversed loading tests are used.

The proposed corrected mean strain model (9) can also be used for representing the LCF curve in the form of Coffin – Manson [24] and Weibull [25] equations. The model applicability is limited to the range of fatigue life where the model was constructed.

Test results considered

To estimate the quality and compare different models of correcting for mean stresses and strains, the LCF test results for smooth specimens made from Ti-6Al-4V ELI alloy [26, 27] and an Iron-based alloy [17] were used. The tests were conducted according to ASTM E606 [28] at room temperature for both the strain-controlled fully-reversed and mean strain loading cycles. In the test data the number of cycles to failure was in the range of $\sim 10^2 - 10^5$. Tables 1 and 2 show the analysis input data. In Table 1 the maximum stress value σ_{max} for the Ti-6Al-4V ELI alloy was determined as the sum of the stress amplitude σ_a and the mean cycle stress σ_m, $\sigma_{max} = \sigma_a + \sigma_m$. For the Iron-based alloy the elasticity modulus had the constant value of E = 189.6 GPa [17].

Model verification

This section considers the results of constructing strain-life LCF curves using the proposed mean strain correction model (10) and compares this model to the SWT (3) and Walker (5) mean stress correction models. For constructing the SWT model the results of fully reversed testing of specimens were used, while the Walker and the model proposed utilized all test results. To evaluate the quality of the regression models, the standard deviation of the logarithm of the number of cycles to failure (SD) and the coefficient of determination (R^2) were used. To simplify the representation of statistical parameters of the models, it was assumed that the number of cycles to failure is governed by the log-normal distribution, while the mean deviation of the logarithm of the number of cycles to failure is constant in all the considered range. The predicted life N_p is compared to the number of cycles to failure, which is demonstrated

Table 1. Results of testing Ti-6Al-4V ELI [26, 27] specimens

R_ε	$\Delta\varepsilon$, mm/mm	σ_{max}, MPa	E, GPa	Cycles to failure
Fully-reversed tests				
–1	0.02	741	107	1880
–1	0.02	698	105	1993
–1	0.02	728	105	2270
–1	0.016	677	106	6457
–1	0.016	690	108	7169
–1	0.014	759	106	24,587
–1	0.014	761	106	24,906
–1	0.012	678	108	62,476
–1	0.012	644	105	64,025
–1	0.012	663	105	103,805
Mean strain tests				
–0.5	0.018	777	106	5258
–0.5	0.018	779	107	5773
–0.5	0.015	792	106	11,350
–0.5	0.015	803	107	11,496
–0.5	0.012	827	106	64,124
0	0.02	778	107	2732
0	0.02	779	105	3362
0	0.016	849	103	5699
0	0.016	761	105	6996
0	0.012	831	105	28,646
0	0.012	838	106	32,736
0.5	0.009	906	105	32,033
0.5	0.009	864	107	49,394
0.5	0.008	922	106	64,961
0.5	0.008	883	105	115,442

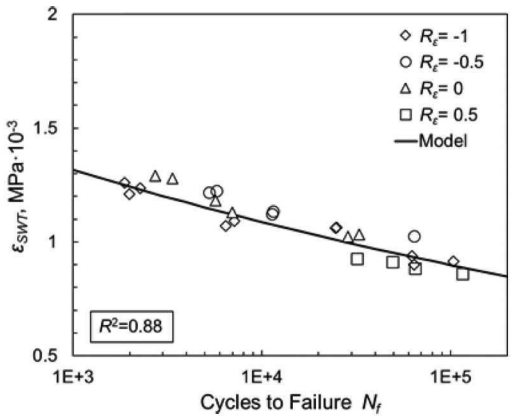

Fig. 2. Equivalent SWT strain versus cycles to failure for Ti-6Al-4V ELI alloy

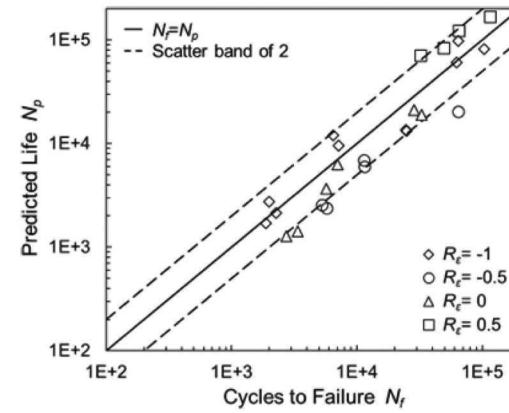

Fig. 3. Comparison between cycles to failure and predicted life using SWT model for Ti-6Al-4V ELI alloy

Table 2. Results of testing Iron-based [17] specimens

R_ε	Δε, mm/mm	σ_{max}, MPa	Cycles to failure
	Fully-reversed tests		
–1	0.006	490	10,223
–1	0.006	536	10,396
–1	0.006	546	8180
–1	0.0097	808	605
–1	0.01	763	672
–1	0.01	778	642
–1	0.015	875	209
–1	0.015	876	340
	Mean strain tests		
0	0.006	804	3958
0	0.006	856	3895
0	0.00597	815	3919
0	0.006	885	4050
0	0.006	845	2470
0	0.004	734	16,388
0	0.00393	703	22,896
0	0.004	704	15,388
0	0.004	646	38,648
0	0.004	698	11,960
0.6	0.0075	961	1099
0.6	0.0075	947	1544
0.6	0.0075	779	966
0.6	0.005	858	4665
0.6	0.005	969	4342
0.6	0.005	954	4240
0.6	0.004	1089	7460
0.6	0.004	1007	11,134
0.6	0.004	821	10,876

by the estimation error. On the diagrams the calculation error is visualized with scatter bands with a

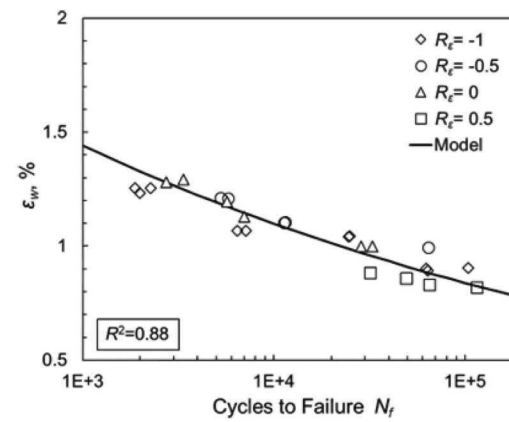

Fig. 4. Equivalent Walker strain versus cycles to failure for Ti-6Al-4V ELI alloy

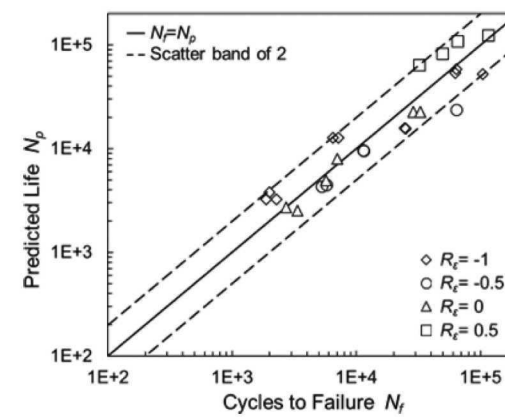

Fig. 5. Comparison between cycles to failure and predicted life using Walker model for Ti-6Al-4V-ELI alloy

factor of two. The experimental points above the upper band indicate that the estimate is conservative, while the experimental points below the lower band indicate that the estimate is conservative.

Figures 2 – 7 show the relationship of equivalent strain vs. N_f and compares N_p and N_f for the

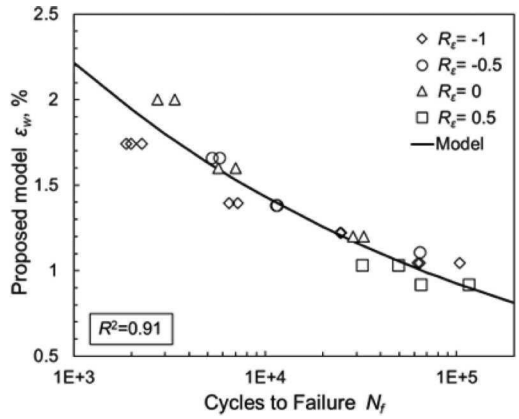

Fig. 6. Proposed equivalent strain (10) versus cycles to failure for Ti-6Al-4V-ELI alloy

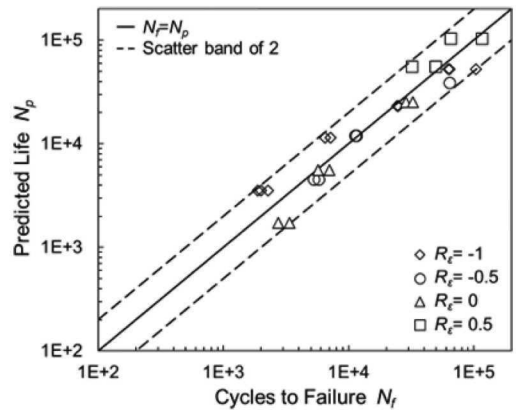

Fig. 7. Comparison between cycles to failure and predicted life using the proposed model (10) for Ti-6Al-4V ELI alloy

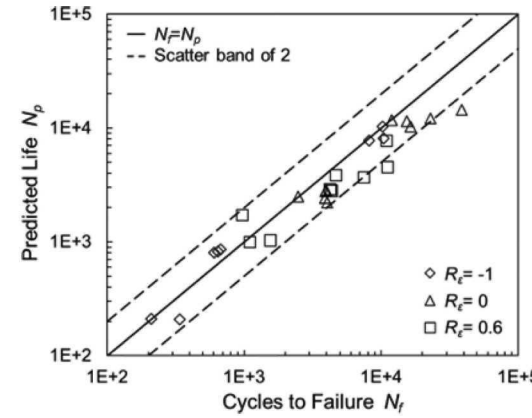

Fig. 8. Comparison between cycles to failure and predicted life using SWT model for iron-based alloy

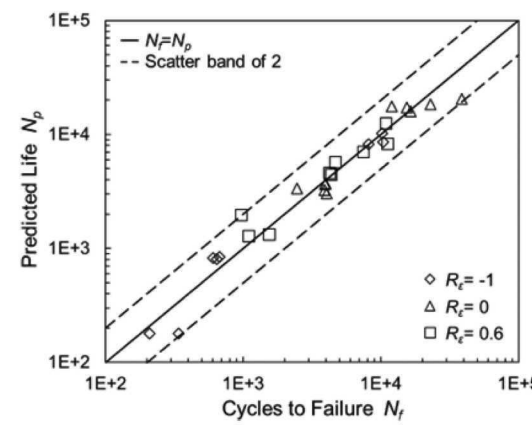

Fig. 9. Comparison between cycles to failure and predicted life using Walker model for iron-based alloy

Ti-6Al-4V ELI alloy. It is seen that four points lie below the lower band for SWT model and one point lie below the lower band for Walker model. The proposed model performs somewhat better compared to the SWT and Walker models because all points are within the error band. Also the statistical estimate of the modeling results indicates that the quality of the proposed regression model is better than for SWT and Walker models (Table 3). However, it should be noted that none of the models give a conservative life estimate for the case of positive strain ratio for the number of cycles to failure $\sim 10^4 - 10^5$. SWT and Walker models yield close results because the Walker constant in model (5) was 0.56, which is close to the value of 0.5.

Figures 8 – 11 compares N_p and N_f for the Iron-based alloy and show the relationship of proposed equivalent strain (10) vs. N_f and compares N_p and N_f for the Iron-based alloy. It is seen that the SWT model is more conservative and less accurate than the Walker model and the model (10) proposed in this paper. For the SWT model, three points were below the lower error band, while only one point

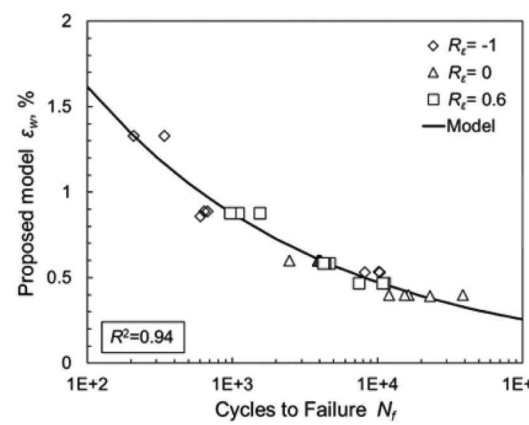

Fig. 10. Proposed equivalent strain (10) versus cycles to failure for iron-based alloy

was below the lower error band for the Walker model and the model proposed. The SD value of the Walker model and the model proposed is much less than that of the SWT model (see Table 3). The re-

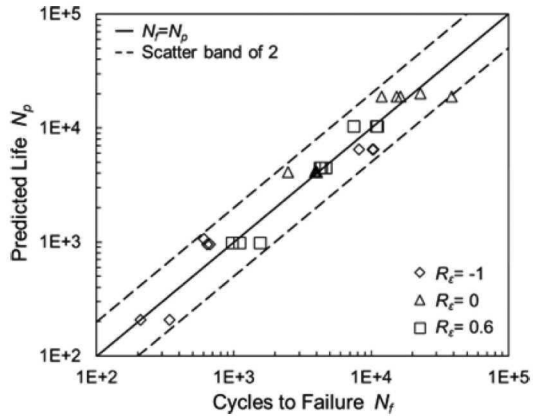

Fig. 11. Comparison between cycles to failure and predicted life using proposed model (10) for Iron-based alloy

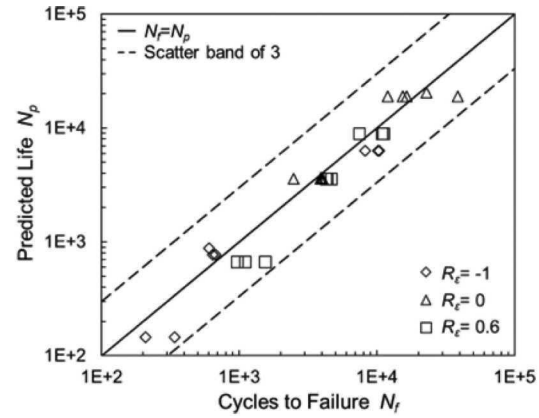

Fig. 13. Comparison between cycles to failure and predicted life using model (12) for iron-based alloy

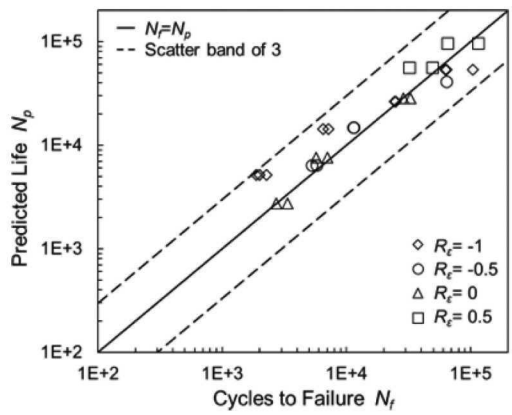

Fig. 12. Comparison between cycles to failure and predicted life using model (12) for Ti-6Al-4V ELI alloy

sults obtained by the Walker model and the model proposed are close to each other.

The presented results of model (10) verification exhibit an acceptable model quality and life prediction accuracy.

Proposed model to be used with a limited amount of experimental data

The analysis of thermal and stress state of aviation gas turbine engines' critical parts made from titanium, iron and nickel alloys, for example, discs and shafts, indicates that most stress concentration zones generally have a cycle with a positive strain ratio. In rare cases, the cycle has a negative strain ratio. In materials' testing for engine parts, LCF characteristics are determined based on strain-controlled $R_\varepsilon = -1$ or $R_\varepsilon = 0$ tests. If a material has only the results of $R_\varepsilon = 0$ tests, the model can be built and estimation of fatigue life considering positive and negative strain ratios can be done based on proposed model (9) with $w_\varepsilon = 0.8$

$$\varepsilon_w = \Delta\varepsilon\left(\frac{1}{1-R_\varepsilon}\right)^{0.2}. \qquad (12)$$

The selection of the exponent in Eq. (12) is justified by the fact that the Walker constant in model (10) is $w_\varepsilon = 0.82 - 0.83$ for both the Ti-6Al-4V ELI and Iron-based alloy. The proposed model (12) is of practical interest for predicting fatigue life of critical parts of gas turbine aviation engines when there is limited experimental data. This is an advantage over the SWT model based on fully reversed test results.

The comparison of N_p with N_f for the Ti-6Al-4V ELI and Iron-based alloy specimens using model (12) showed satisfactory results of fatigue life prediction (Figs. 12 and 13). All points lie within the error band of three. The statistical estimate of modeling results showed acceptable model quality (see Table 3). For both materials, SD ≤ 0.2 and $R^2 > 0.9$.

CONCLUSIONS

This paper proposed a Walker-based mean strain correction model (9) for LCF life prediction of high loaded parts. The model is based on a func-

Table 3. Statistical parameters and Walker constants

Alloy	SWT (3)		Walker (5)			Proposed (10)			Proposed (12)	
	SD	R^2	w	SD	R^2	w_ε	SD	R^2	SD	R^2
Ti-6Al-4V ELI	0.27	0.88	0.56	0.20	0.88	0.82	0.17	0.91	0.20	0.91
Iron-based	0.20	0.94	0.60	0.13	0.95	0.83	0.15	0.94	0.16	0.94

tion depending on the strain range and strain ratio controlled in the strain-controlled LCF test and a constant reflecting the material sensitivity to the strain cycle strain ratio. The advantage of the model is its independence from the stress cycle parameters which can change during the strain-controlled LCF test. The model was verified based on results of LCF strain-controlled testing at room temperature of smooth Ti-6Al-4V ELI and Iron-based alloy specimens. The results of verification and comparison with conventional SWT and Walker models considering mean stress effect exhibited an acceptable result of fatigue life prediction. For titanium alloy the proposed model showed the best prediction accuracy. The limitation of the model is the pure compression condition when $\varepsilon_{max} \leq 0$.

A model (12) for predicting fatigue life of aeroengine' critical parts based on a limited amount of experimental data is also proposed. The model is constructed based on results of strain-controlled $R_\varepsilon = 0$ tests with just two arguments: strain range and strain ratio. The statistical estimate of the modeling results of predicting fatigue life of Ti-6Al-4V ELI and Iron-based alloys also indicated that the quality of the proposed model is satisfactory.

Conflict of interest statement

The author declares no conflict of interest.

REFERENCES

1. American Society for Testing and Materials. ASTM E739-10 (2015), Standard Practice for Statistical Analysis of Linear or Linearized Stress-Life (S-N) and Strain-Life (ε-N) Fatigue Data. ASTM International, West Conshohocken, PA, 2015.
2. **Socie D. F., Morrow J.** Review of Contemporary Approaches to Fatigue Damage Analysis / Risk Fail Anal. Improv. Perform. Reliab. 1980. P. 141 – 194.
3. **Smith K., Watson P., Topper T. H.** A Stress-Strain Function for the Fatigue of Metals / J. Mater. JMLSA. 1970. N 5. P. 767 – 778.
4. **Walker K.** The Effect of Stress Ratio During Crack Propagation and Fatigue for 2024-T3 and 7075-T6 Aluminum / Eff. Environ. Complex Load Hist. Fatigue Life. March 1970. P. 1 – 14.
5. **Manson S. S., Halford G. R.** Practical implementation of the double linear damage rule and damage curve approach for treating cumulative fatigue damage / Int. J. Fract. 1981. Vol. 17. P. 169 – 192.
6. **Lorenzo F., Laird C.** A new approach to predicting fatigue life behavior under the action of mean stresses / Mater. Sci. Eng. 1984. N 62. P. 205 – 210. DOI: 10.1016/0025-5416(84)90223-4
7. **Ince A., Glinka G.** A modification of Morrow and Smith — Watson — Topper mean stress correction models / Fatigue Fract. Eng. Mater. Struct. 2011. N 34. P. 854 – 867. DOI: 10.1111/j.1460-2695.2011.01577.x
8. **Yuan X., Yu W., Fu S., et al.** Effect of mean stress and ratcheting strain on the low cycle fatigue behavior of a wrought 316LN stainless steel / Mater. Sci. Eng. A. 2016. N 677. P. 193 – 202. DOI: 10.1016/j.msea.2016.09.053
9. **Ince A.** A mean stress correction model for tensile and compressive mean stress fatigue loadings / Fatigue Fract. Eng. Mater. Struct. 2017. N 40. P. 939 – 948. DOI: 10.1111/ffe.12553
10. **Bergman J., Seeger T.** On the influence of cyclic stress-strain curves, damage parameters and various evaluation concepts on the life prediction by the local approach. In: Proceedings of the 2nd European Conference on Fracture, Darmstadt, Germany. VDI-Report of Progress. Vol. 18. 1979.
11. **Dowling N. E.** Mechanical Behavior of Materials. — Prentice Hall, 2012.
12. **Nihei M., Heuler P., Boller C., Seeger T.** Evaluation of mean stress effect on fatigue life by use of damage parameters / Int. J. Fatigue. 1986. N 8. P. 119 – 126. DOI: 10.1016/0142-1123(86)90002-2
13. **Kujawski D.** A deviatoric version of the SWT parameter / Int. J. Fatigue. 2014. Vol. 67. P. 95 – 102. DOI: 10.1016/j.ijfatigue.2013.12.002
14. **Theodore N.** High Cycle Fatigue: A Mechanics of Materials Perspective. — Elsevier Science, 2006.
15. **Lu S., Su Y., Yang M., Li Y.** A Modified Walker Model Dealing with Mean Stress Effect in Fatigue Life Prediction for Aeroengine Disks / Math. Probl. Eng. 2018. DOI: 10.1155/2018/5148278
16. **Chang L., Ma T. H., Zhou B. Bin, et al.** Comprehensive investigation of fatigue behavior and a new strain-life model for CP-Ti under different loading conditions / Int. J. Fatigue. 2019. Vol. 129.105220. DOI: 10.1016/j.ijfatigue.2019.105220
17. United States & Battelle Memorial Institute. MMPDS-07: Metallic materials properties development and standardization (MMPDS). — Washington, D.C.: Federal Aviation Administration. 2012.
18. **Corran R. S. J., Williams S. J.** Lifing methods and safety criteria in aero gas turbines / Eng. Fail Anal. 2007. N 14. P. 518 – 528. DOI: 10.1016/j.engfailanal.2005.08.010
19. **Dua D., Vasantharao B.** Life Prediction of Power Turbine Components for High Exhaust Back Pressure Applications: Part I — Disks / Proc. ASME Turbo Expo. 2015. 7A. DOI: 10.1115/GT2015-43333
20. **Golowin A., Denk V., Riepe A.** Probabilistic Damage Tolerance Methodology for Solid Fan Blades and Disks / Int. J. Aerospace Mech. Eng. 2016. N 10. P. 932 – 937. DOI: 10.5281/zenodo.1124413
21. **Dowling N. E., Calhoun C. A., Arcari A.** Mean stress effects in stress-life fatigue and the Walker equation / Fatigue Fract. Eng. Mater. Struct. 2009. Vol. 32. P. 163 – 179. DOI: 10.1111/j.1460-2695.2008.01322.x
22. **Dowling N. E.** Mean stress effects in strain — life fatigue / Fatigue Fract. Eng. Mater. Struct. 2009. Vol. 32. P. 1004 – 1019. DOI: 10.1111/j.1460-2695.2009.01404.x
23. **Servetnik A. N.** A modified Walker model for constructing a low cycle fatigue curve with mean strain effect / Aviation Engines. 2020. N 1(10). P. 39 – 46.
24. **Manson S. S., Hirschberg M. H.** Fatigue: An Interdisciplinary Approach. — Syracuse: Syracuse University Press, 1964.
25. **Weibull W.** Fatigue testing and analysis of results. — London: Pergamon Press, 1961.
26. **Carrion P. E., Shamsaei N.** Strain-based fatigue data for Ti-6Al-4V ELI under fully-reversed and mean strain loads / Data Brief. 2016. N 7. P. 12 – 15. DOI: 10.1016/j.dib.2016.02.014
27. **Carrion P. E., Shamsaei N., Daniewicz S. R., Moser R. D.** Fatigue behavior of Ti-6Al-4V ELI including mean stress effects / Int. J. Fatigue. 2017. Vol. 99. P. 87 – 100. DOI: 10.1016/j.ijfatigue.2017.02.013
28. ASTM E606/*E*606M-12. Standard test method for strain-controlled fatigue testing. — West Conshohocken, PA: ASTM International, 2012.